# Calculation of global properties of a multi - layered solid wood structure using Finite Element Analysis

Guillermo Zafra-Camón

Abstract

# Calculation of global properties of a multi-layered solid wood structure using Finite Element Analysis

*Guillermo Zafra-Camón*

Finite Element Method (FEM) is a powerful numerical tool which, combined with the fast development of Computer Science in the last decades, had made possible to perform mechanical analysis of a wide range of bodies and boundary conditions.

However, the complexity of some cases may turn the calculation process too slow and sometimes even unaffordable for most computers. This work aims to simplify an intricate system of layers with different geometries and material properties by approximating it through a homogeneous material, with unique mechanical parameters. Besides the Finite Element analysis, a theoretical model is created, in order to understand the basis of the problem, and, as a first approach, check whether the assumptions made in the FEM model are acceptable or not.

This work intends to make a small contribution to the understanding of the mechanical behaviour of the Vasa vessel, which will eventually lead to the design of a new support structure for the ship. The preservation of the Vasa is a priority for the Swedish Property Board, as it is one of the main monuments of Sweden.

Keywords: finite elements, wood mechanics, homogenization of solids, multi-layered solid

# Preface

This thesis is a contribution to the overall Vasa project, a larger project that involves a number of sub-groups from different fields. It involves two parts that cooperate together to make it possible: the Vasa Conservation Council and a group of researchers within several areas as Mechanics or Chemistry.

These people from the Applied Mechanics division at Uppsala University are the main participants: Kristofer Gamstedt (Project Coordinator), Ivón Hassel (Associate Professor), Nico Van Dijk (Post Doc.), Inghela Bjurhager (Assistant Professor), Reza Afshar (Post Doc.), Alexey Vorobyev (PhD student), Dan Wu (PhD Student), and Claudia Varas Torres (BsC Thesis worker).

# Table of contents

# 1. Introduction

The aim of this thesis is representing the complex assembly structure of the Hull as a homogeneous element for its future use in a simplified global computer model of the whole Ship. To achieve this goal is important to study the mechanism of load transference through the layered structure of the hull. The mechanical properties of each element constituent of the layered structure need to be characterized, in order to finally determine the global parameters of the composed layered structure.

The mechanical modelling of the ship is a complex task, which requires a study of the different parts of the vessel and its connections, but this work scopes to analyse one part of the ship, which the purpose of adding one more piece of the puzzle necessary for understanding the whole case.

This study will be done by a combination of methods, such as a theoretical mechanical analysis, and Finite Element (FE) simulations. This work is intended to contribute to the understanding of the behaviour of the Vasa hull, in particular the mechanical properties of its hull as a composite structure. Eventually, the outcome of the Vasa project will lead to a better knowledge of the interaction of the Vasa vessel and its support structure, which will be replaced in the future in order to advantage the preservation of the ship.

Laboratory tests were programmed and samples were already manufactured, but eventually, due to equipment and logistic limitations, were not able to be performed by the time of completion of this work. However, it is expected these tests will be done in the future, so they would be compared with the results obtained in this text.

## 2. Background

The Vasa warship construction started in 1626, under the reign of Gustav Adolf II. The vessel is 69 metres long, with a height of 52.3 metres, and a width of 11.7 metres, which were quite great dimensions for a 17$^{th}$ century warship, due to The King's desire of producing a symbol of Sweden's supremacy.

It was finally launched in a Stockholm's dock on August 10$^{th}$, 1628. However, the ship sunk quite fast because it was too svelte, and its centre of gravity was placed too high. These facts severely affected the stability of the vessel.

A long time after the occurrence, in 1956, A. Franzén (a marine technician), studied the possibility of refloating the Vasa from its wreck site [1]. After some investigations, the sunken vessel was located standing up deep in the Baltic Sea near Stockholm's Archipelago. The ship was rescued, and today rests at the Vasamuseet, in the island of Djurgården. The museum was built around the ship, and opened at the beginning of the nineties. Today it is the best preserved 17$^{th}$ century warship, and its museum one of the most popular in Sweden, therefore its conservation is a priority for the Swedish authorities.

Despite of being in the ocean for more than three hundred years, the ship called Vasa was found quite well conserved, due to a number of reasons, such as the low concentration of salts in the water (impeding the proliferation of wood eating organisms), the low water temperature, the lack of oxygen, and the high performance of the oak wood [2].

The restoration work started with the substitution of the ironed elements, severely affected by corrosion. Then, the wood was treated with polyethylene glycol (PEG), as well as boric and borax acid to prevent from fungus attack. However, this treatment has provoked an increase of the fragility of the wood, which constitutes even nowadays a big problem for the conservation of the vessel.

In order to prevent its degradation, the ambient conditions were controlled, but despite all the efforts, displacement measurements showed that the deformation of the ship is considerable; this is why a new support structure (the current one was built in the 1960s), that takes into account the mechanical behaviour of the interaction structure-hull, is needed.

The wood of the Vasa vessel is modified oak, specifically *Quercus Robur* (which will be called Vasa oak from now). Wood is an orthotropic material, with its mechanical properties varying according to three main perpendicular axes. The ship's hull structure is composed of three layers of boards, with a complex system of joints supporting the decks, and linking different parts of

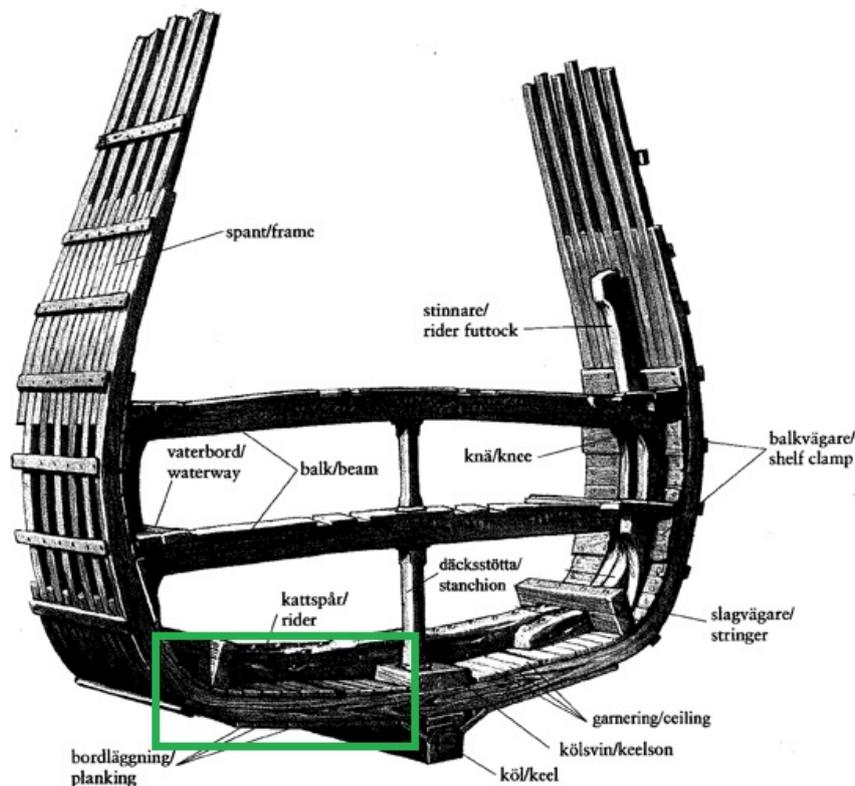the structure [3]. The different components of the basic structure of the ship are depicted in figure 1.



Figure 1. Credits: Vasamuseet

The hull, which is the part of the vessel that is being analysed in this text, is a multi-layer dowelled timber structure. It is composed by oak boards which form three layers, called planking, frame and ceiling [4]. The frame's main fibres' direction is oriented orthogonally respect to that of the planking and ceiling elements. They are all joined by wooden dowels (trunnels) and bolts, whose diameter is slightly greater than the diameter of the hole, which makes the layers remain bonded. A scheme of the hull (the front view of the green section marked in figure 1) can be seen in figure 2.
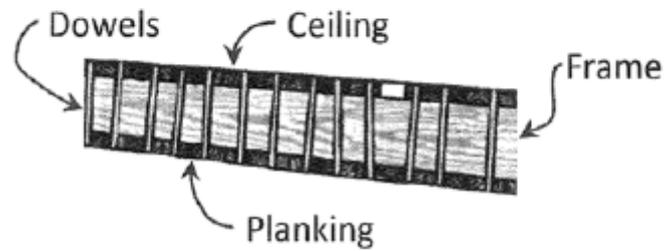
Figure 2: Vasa hull cross – section. Credits: Vasamuseet

The assembly presents a [0/90/0] angle disposition cross-layer fibre orientations. In other words, the frame is rotated 90 degrees around the bolts and dowels direction axis respect to the planking and the ceiling.

In the Vasa, the original bolts are quite damaged, therefore they are being progressively replaced (see figure 3), as the corroding iron is harming the hull, and speeding its degradation. Approximately 5000 bolts are being substituted [2][5], since the process started in the summer of 2011.These new replacements are manufactured in stainless steel by the company Sandvik.



Figure 3: new and old bolts. Credits: Sandvik

Once the works are completed, those bolts will be the main agent that will keep the hull's layers together, thus they are considered when studying the mechanical response of the hull in this text.

## 2.1. Parameters involved in the development of the mechanical model

In order to determine the global mechanical properties of a layered composite (whose properties are represented with an orthotropic material model), it is very important to study three parameters of each individual components. These are: Young's moduli (E), shear moduli (G), and Poisson's ratios (v) along three main directions. Their formulation and explanation is [6] is:

- Young's modulus: also known as tensile modulus, it measures the force per unit area that is required to either stretch or compress the material along the axis where the load is applied. Thus, it is an indicator of the stiffness.

$$E = \frac{\sigma}{\varepsilon} \tag{1}$$

- Shear modulus: is the quotient of the shear stress (parallel to the plane the force is applied on) divided by the shear strain (the change in angle provoked by the mentioned load).

$$G = \frac{\tau}{\gamma} \tag{2}$$

- Poisson's ratio: it is defined as the negative ratio between the transverse strain to the axial strain (figure 4), having uniaxial stress load.

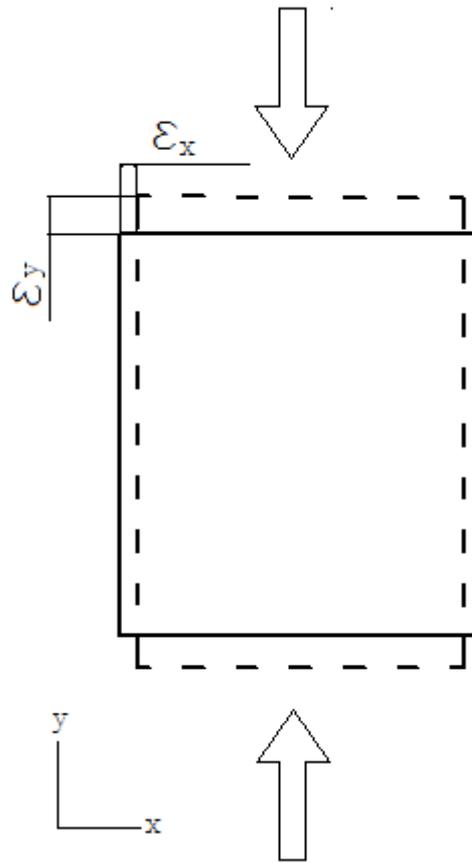$$v = -\frac{\varepsilon x}{\varepsilon y} \tag{3}$$

Figure 4: obtention of Poisson's ratio

where σ is the compression stress (tensile stress could had been applied too, but with compression it is ensured that the layers of the composite will remain bonded in any case), ε is the longitudinal strain, $\tau$ is the shear stress, $\gamma$ is the shear deformation, and $\varepsilon_x$ and $\varepsilon_y$ are the transverse and axial strains (which are the ratio between length change per unit length, along the transverse and axial direction, respectively).

FE of geometrically complex structures, in terms of geometry and loads, amongst other parameters, carries difficulty of computation due to the large amount of data involved. The most critical factors are:

- Geometry
- Boundary conditions
- Loads

The simplicity of these parameters can dramatically affect the calculation in terms of time (which can be important when having a big amount of data), accuracy and convergence of the solution.

For instance, a complex geometry requires a very fine mesh, which means the number of equations to solve increase in the same proportion.

A comprehensive and detailed control of these parameters will eventually facilitate the design a future tractable model of the hull, which will be built by reproducing the *super-element*. In consequence, the manageability of the model will depend on the simplicity of the mentioned element.

## 2.2. Homogenization process

The concept of *homogenization,* applied to this case of study, consists of obtaining a uniform element, with singular mechanical properties, starting from a composite that has different parts which have different characteristics.

The goal of doing this simplification is to have unique, but still representative, values for the whole element, which can be used for future models of the whole vessel. An additional advantage is the geometry becomes continuous, which reduces the number of necessary nodes and, therefore, the number of equations.

That aim is reached by performing simulations of the original heterogeneous element and analysing its mechanical response as a whole. The desired parameters (E, G, and v) are obtained with different methods, which are detailed in the coming chapters.

A scheme of the *homogenization* idea is shown in figure 5: from a composite with different material properties (indicated with subscripts P for the planking and ceiling, F for the frame, and B for the bolt, along the directions indicated in the same figure), an approximation of those properties along the three main directions for a homogeneous element is calculated by combining the mechanical response of every component. The way of combine them varies for each method.
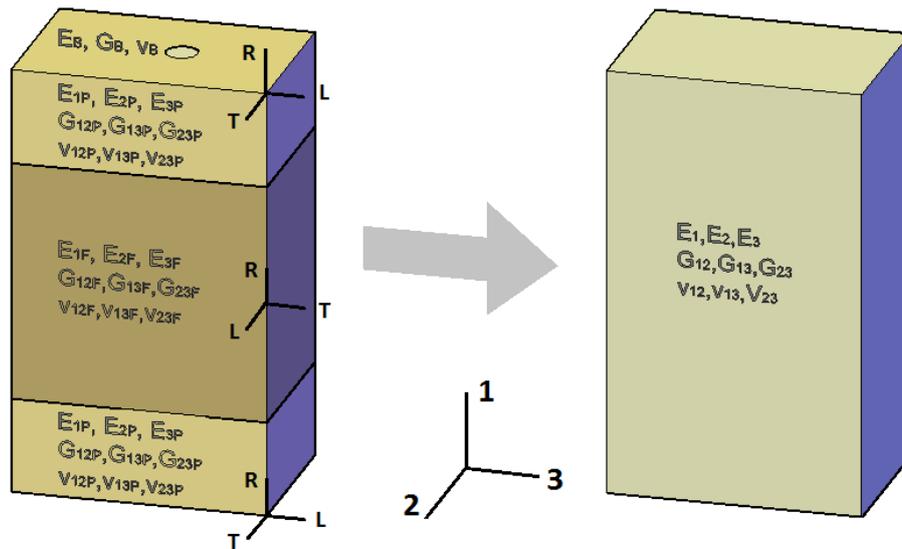
Figure 5: Scheme of the homogenization of the composite by estimating its global properties

In the same figure, both local (L, T, and R), and global coordinates (1, 2, and 3) are displayed. The local axis correspond to the wood fibre directions, which can be seen in figure 6: longitudinal (L), tangential (T), and radial (R).
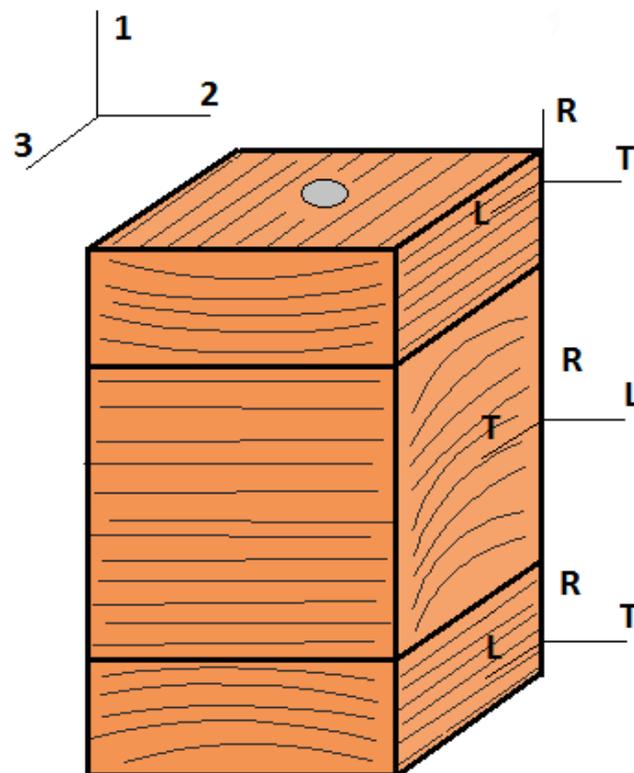


Figure 6: wood fibre directions

The representative element, named from now on *super-element*, should be computational affordable, and reflect the mechanical behaviour of the hull as close to reality as possible. It must be stated that, due to the limitations of a non-empirical model, the final result is not exact. For this reason, the approximation shown in figure 4 was estimated using two different procedures: a theoretical model using concepts of mechanics, and Finite Element Analysis (FEA), in order to compare the obtained values for each one. Also experimental tests will be done by Claudia Varas. Using different methodologies allows to obtain some values that are not possible to obtain experimentally due to the lack of either equipment or material, as well as to corroborate the calculated results.

A first approximation of this *super-element* was already proposed by Hurtado Sierra and Muñoz García [1]. In their work, a FE model of the hull composite was subjected to certain loads, with the purpose of obtaining the global moduli, which is also the goal of this work. However, a limitation of their procedure is the loads are applied in the surface by using a rigid plate, thus the different components of the hull are joined together and cannot displace relatively where the force is applied, unlike the actual state is. Thus, starting from their idea, and trying to set a more significant boundary conditions, a model for the concrete geometry of this case was developed and analysed.

# 3. Materials and methods

As stated before, the mechanical properties $E_i$, $G_{ij}$, $v_{ij}$ (i = 1, 2, 3), of the case of study composite are calculated in two different ways:

1) Estimation of theoretical values of the parameters (mechanical model): this is a very particular case (solid timber setup in different axis directions joined by specially designed metal bolts); hence it is more desirable to find out a way to calculate it, instead of using any existing method. Once reached this point, there are two options: a) trying to adapt one of the methods that other investigated in already, like Whitcomb [7] (the difference is in this case there is a bolt along the out-of-plane direction of the composite), or b) finding an approximation of the parameters by using the basic concepts of composite laminated materials.

Choosing the option b), the rule of mixtures [6] can be used for estimating composite material properties. However, we often need better methods. The validity or not of this mechanical model will be checked once compared with the results in the other two ways (replica tests and FE).

2) Finite element (FE) simulations: the goal of the thesis is to find the *super-element*, but not to use it to perform simulations of the whole ship (that will be a proposed future work). Hence, once the mechanical properties are obtained, the necessary FE parameters (type of element, meshing,...) will be set. Then, simulations with the *super-element* will be performed in order to check the actual behaviour is between the limits of the expected.

If this does not happen, the model can be reviewed and modified if necessary, resulting in an iterative process until results match, always taking into account the validity of the hypothesis and simplifications made.

Forth, these two methods are analysed and explained in detail.

## 3.1. Theoretical model

The rule of mixtures is an acceptable first approximation for estimating composite material properties. However, we often need better methods. The accuracy of this mechanical model was later checked once compared with the results with the Finite Element analysis.

The rule of mixtures establishes that a certain property can be estimated from the properties of the individual elements of the composite, multiplied by its volume fraction. In other words, each component of the composite contributes in proportion to its volume. In case of an isotropic matrix which contains a fibre, the system is analogue to springs connected in parallel or in series when the force is applied along the longitudinal or transverse fibre direction, respectively. For the longitudinal direction, the explanation of this analogy is showed below. For the example, Young's modulus was chosen, but the rule of mixtures is a valid methodology for a generic property.
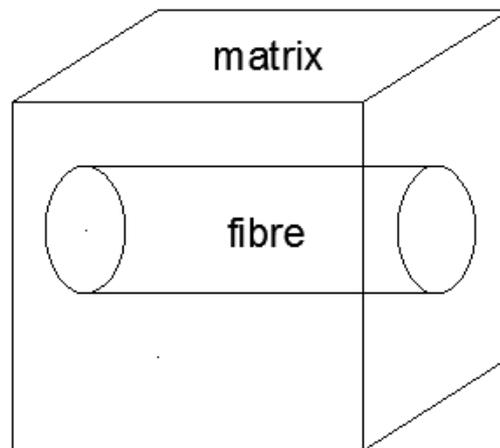


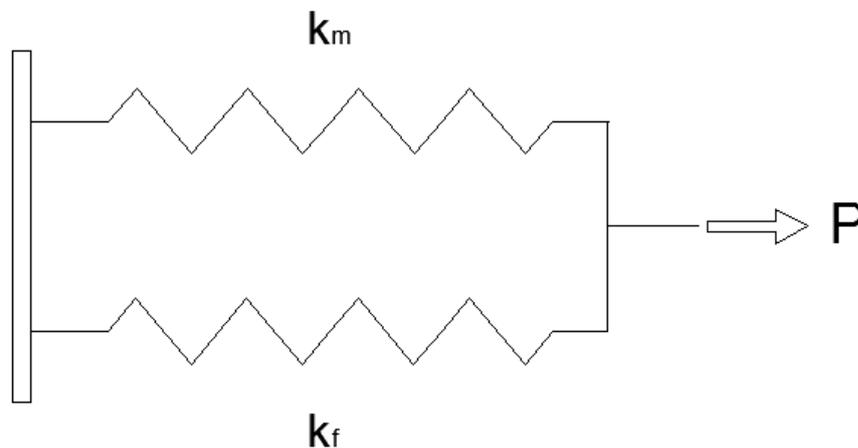Figure 7: isotropic fibre reinforced composite



Figure 8: Spring analogy for an isotropic composite

It is obvious that the displacement ($\delta$) for the matrix and fibre components has to be the same. When a certain load (P) is applied, it is carried partly by the matrix, and partly by the fibre, this is:

$$P = P_f + P_m \tag{4}$$

$$\delta = \delta_f = \delta_m \tag{5}$$

Where subscript $f$ refers to the frame (the central wooden piece) and subscript $p$ refers to the planking and ceiling. Starting from Hooke's law, the value of the applied force P is:

$$\sigma = E \cdot \varepsilon = E \cdot \frac{\delta}{L} = \frac{P}{A} \tag{6}$$

$$P = \frac{\delta \cdot A \cdot E}{L} \tag{7}$$

Where σ is the tension, ε the strain, E the Young's modulus, L the length of the element, and A the cross section area perpendicular to the applied force.

Then, substituting (7) in equation (4):

$$\frac{\delta \cdot A \cdot E_1}{L} = \frac{\delta \cdot A_f \cdot E_f}{L} + \frac{\delta \cdot A_m \cdot E_m}{L} \tag{8}$$

Where $E_1$ is the Young's modulus of the composite along the fibre direction. $A_f$, $E_f$, $A_m$, $E_m$ are the areas and the Young's modulus of the fibre and matrix components, respectively. The areas can be expressed in terms of volumes:

$$A_f = V_f \cdot A \tag{9}$$

$$A_m = V_m \cdot A \tag{10}$$

Finally, combining equations (8), (9), and (10) and simplifying, $E_1$, can be obtained as follows:

$$E_1 = V_f \cdot E_f + V_m \cdot E_m \qquad (11)$$

However, when applying a perpendicular force along a direction perpendicular to the fibres, the methodology should be more sophisticated to be very accurate; nevertheless, good estimations can be obtained if the fibre and the matrix are represented as two springs connected in series (see figure 9).



Figure 9: springs connected in series
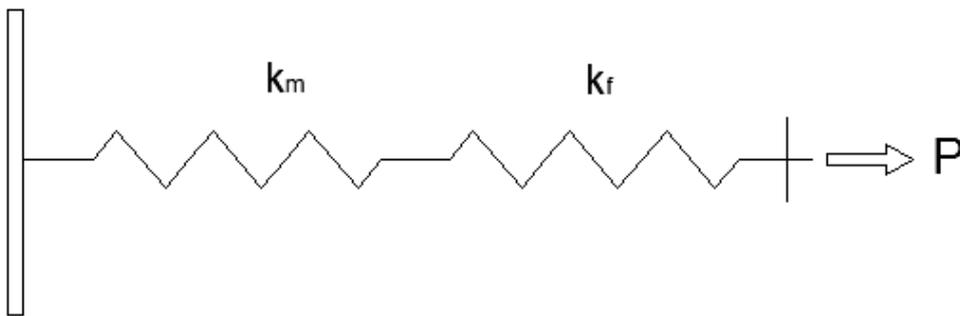
Using this model, the total strain at the point the force is applied is the addition of the deflections suffered by both components (matrix and fibre). Therefore, the final expression for the transverse Young's modulus is:

$$\frac{1}{E} = \frac{Vf}{Ef} + \frac{Vm}{Em} \qquad (12)$$

Which is exactly the expression that is expected to get when two springs are connected in parallel.

For the element of study in this work, an approximation to the moduli was calculated similarly. In this case, the material is orthotropic (except the bolt). First, the sample geometry and material properties are introduced, then the calculation process is explained.

The geometry of the element was determined by the experimental tests samples who were manufactured for future experimental tests for the Vasa team. It consists, as showed in figure 10, in a prism whose dimensions are 385x225x156 mm, composed by two external planks (ceiling and frame), which have a width of 85 mm, and a central piece with a width of 215 mm. They are hold together by a steel bolt, which has a diameter of 28 mm and a thickness of 2 mm.
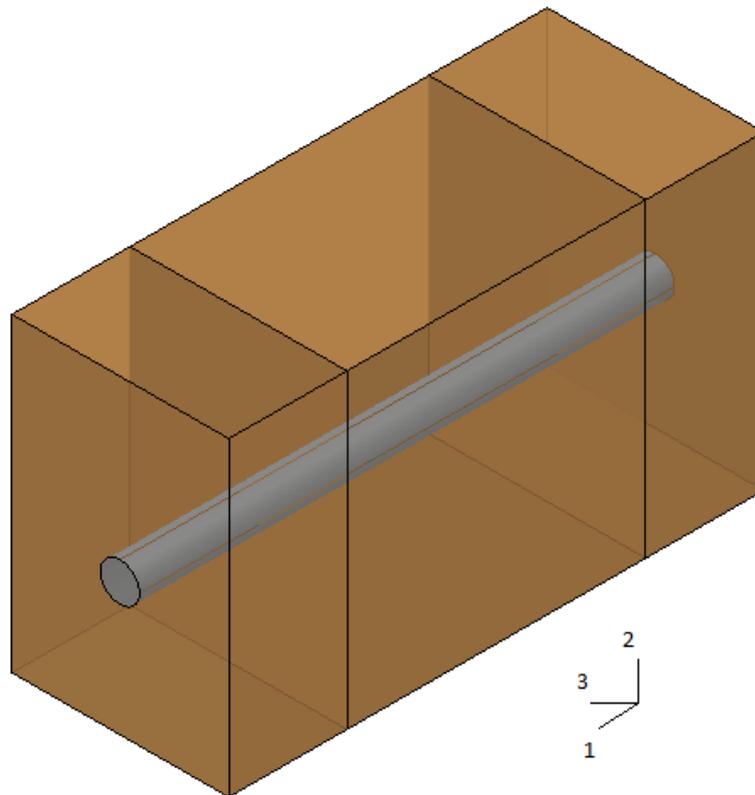


Figure 10: manufactured sample simulating a section of Vasa hull

Detailed drawings (top and front views) of the composite dimensions are shown below in figures 11 and 12.
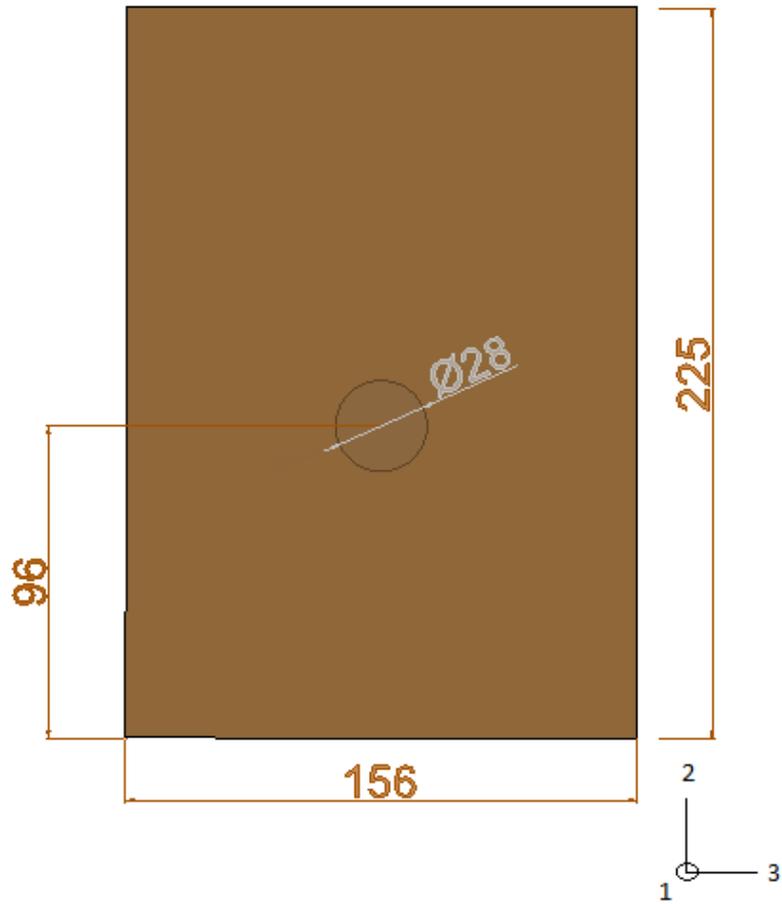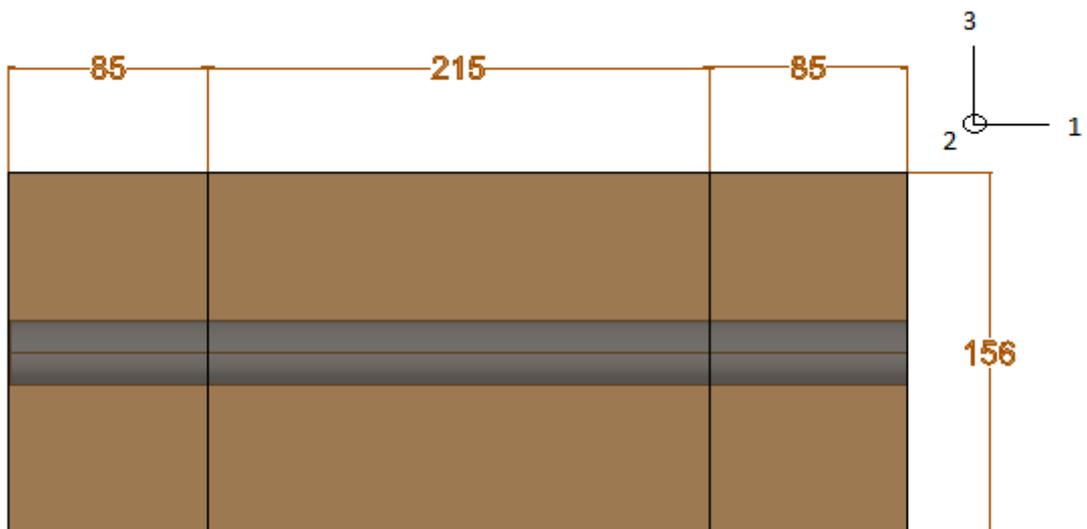
Figure 11: front view



Figure 12: top view

The wooden components of the composite are orthotropic, and the planks have different orientations, therefore, a local coordinate system was defined for each of them. The system's axis were named, based on the fibre direction, as: L, R, and T (longitudinal, radial and tangential).

However, to reference all the composite magnitudes, it was necessary to establish a global coordinate system. These are the global Cartesian axes, named in this case 1, 2, and 3. Both fibre directions and coordinate systems can be seen in figure 6, showed in the previous chapter.

The material properties used for the model are taken from Muñoz and Sierra's work. These values are displayed on table 1. The samples for the laboratory tests are manufactured in *recent oak*; in consequence, these values are used for the theoretical and FE models, therefore all methods can be compared. Once the model is validated, it can be used for Vasa oak, which is the actual wood of the ship.

| | $E_L$ | $E_R$ | $E_T$ | $v_{LR}$ | $v_{RT}$ | $v_{LT}$ | $G_{LR}$ | $G_{LT}$ | $G_{RT}$ |
|---|---|---|---|---|---|---|---|---|---|
| Recent oak | 11,93 | 1,6 | 0,83 | 0,35 | 0,6 | 0,43 | 0,62 | 0,33 | 0,14 |
| Vasa oak | 5,81 | 0,93 | 0,51 | 0,29 | 0,66 | 0,47 | 1,58 | 0,66 | 0,49 |

Table 1: wood material properties

For the bolt, the manufacturing company (Sandvik) gives a value of 197 MPa [8] for E modulus. According to relevant literature about engineering material properties like [9], a Poisson's modulus of 0.27 was set. Then, having those two parameters, shear modulus (G) can be calculated for an isotropic material with equation 13:

$$G = \frac{E}{2 \cdot (1 + v)} \tag{13}$$

which gives a value of 77.56 MPa.

## Estimation of the global parameters (E, G and v)

Subsequently, the rule of mixtures was applied to the case of study, in order to get a theoretical estimation of the global parameters E, G and v (from the stiffness matrix), along the three main directions (1, 2, and 3).

Two different approaches were conducted: *calculation of global stiffness matrix,* which gives values for E, G and v, working with the stiffness matrices. The other method, *calculation of global E moduli*, just calculated for E, consisted of applying the rule of mixtures directly to the Young's moduli.

The reason for using two methods, and giving one of them only values for E moduli, is that this is the most important parameter when looking at the stiffness of the hull, so it is convenient to double check its value. Therefore, after applying both methods, results for E moduli were compared, with the purpose of see if the values for the Young's moduli are similar for both models.

In order to make possible the application of the spring analogy to our sample, the volume was divided in different prismatic parts, as can be seen in figure 14. The bolt (part C) is approximated as a hollow prism (with a thickness of 2 mm, the same the actual bolt has), with the purpose of having a more regular geometry, which facilitates the understanding of the analogy.

Note that the position of the components does not affect the results of estimations using this method, so the bolt was placed in one of the corners to make the decomposition geometrically easier. In addition, the wooden components were also divided in part A and part B (the region under part C), to make the process more clear.

Then, the homogenization was done in different steps, which can be seen in figures 16 to 19. At every step, the rule of mixtures was applied, resulting in new and unique values for the joined parts of the composite. The steps are the same for the two mentioned methods; the only difference is that the target values are E for the first case, and the stiffness matrices components for the second case.
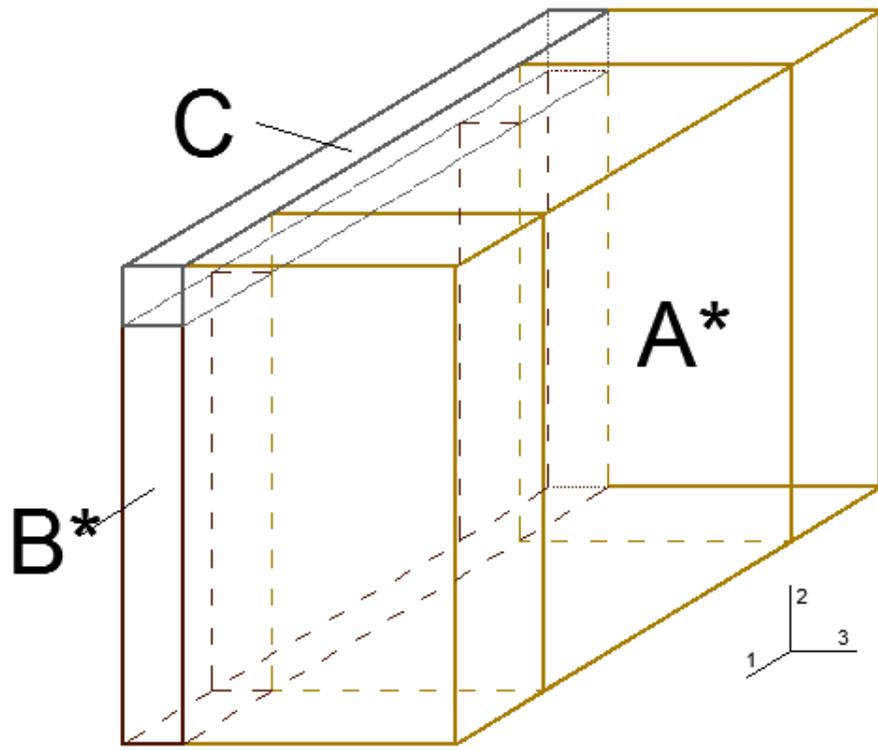
Figure 13: division of the MLSWS in different parts
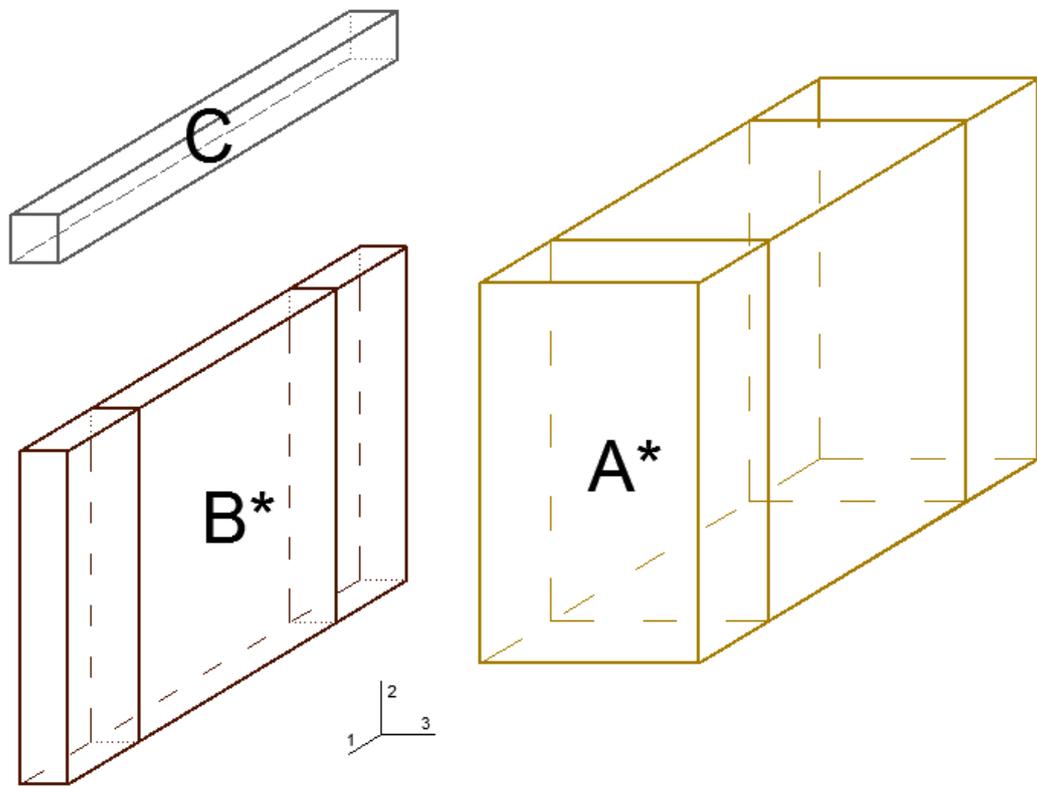


Figure 14: division of the MLSWS in different parts

## Mechanical model: step-by-step process of homogenization

Below, the followed steps of the *homogenization* process of the element are explained and illustrated:

- Step 1: homogenization of wooden parts (A* and B*). For displacements along axis 1, according to the rule of mixtures, the elements are connected in series. For the other directions, they behave like springs in parallel. Thus, using Matlab [10], a loop is created, taking into account that when j = 1, formula for in series has to be used. Else, it is necessary to use formula for elements connected in parallel.



Figure 15: step 1 (I)
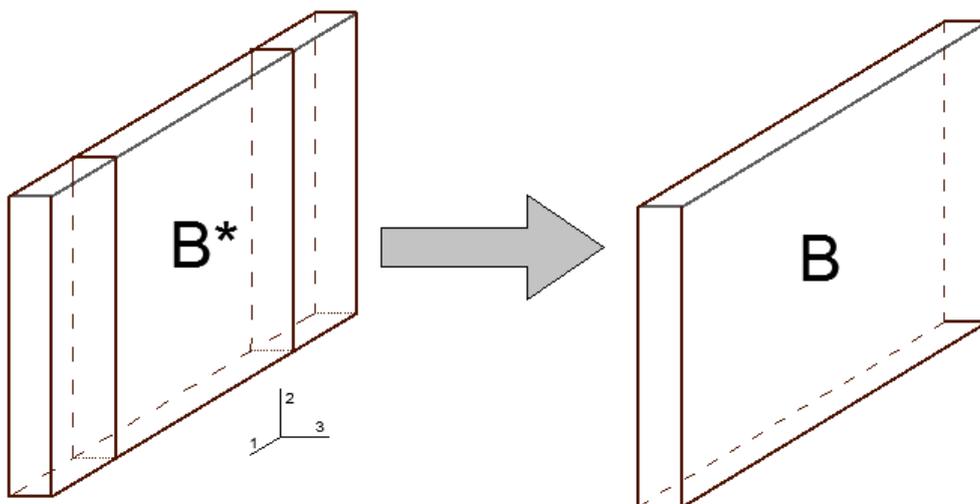


Figure 16: step 1 (II)

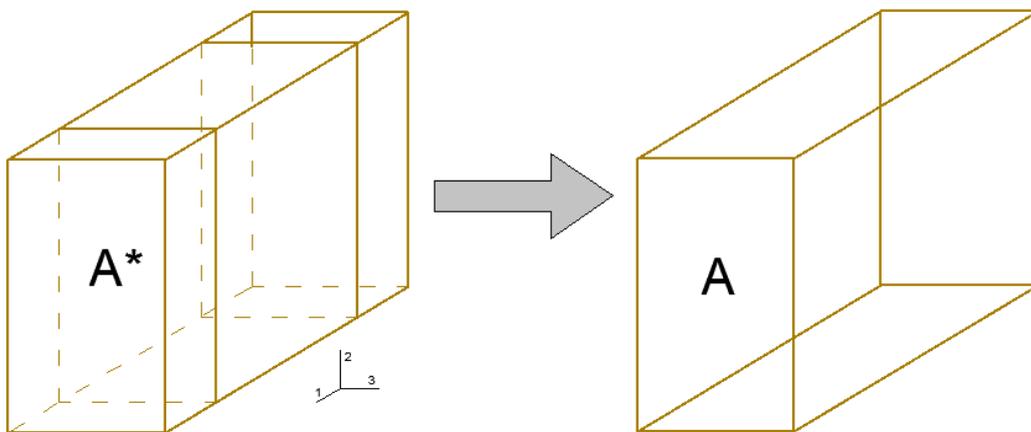- Step 2: homogenization of the bolt. The hollow prism is represented as a solid prism, whose properties (stiffness matrix component or Young's moduli) are multiplied times the proportion of material, this is, times the coefficient thickness of bolt walls over diameter of the whole section.

- Step 3: homogenization of C+B: as can be seen in figure 17, for displacements along axis 1, the elements are connected in series. For the other directions, they behave like springs in parallel. Thus, likewise in step 1, a loop is created, taking into account that when j=1, formula for in series has to be used. Else, it is necessary to use formula for elements connected in parallel.
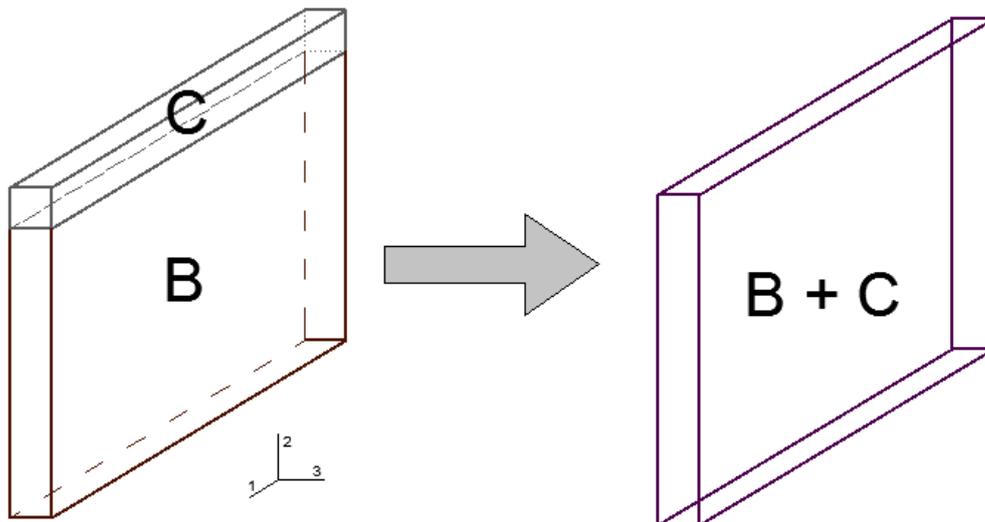


Figure 17: step 3

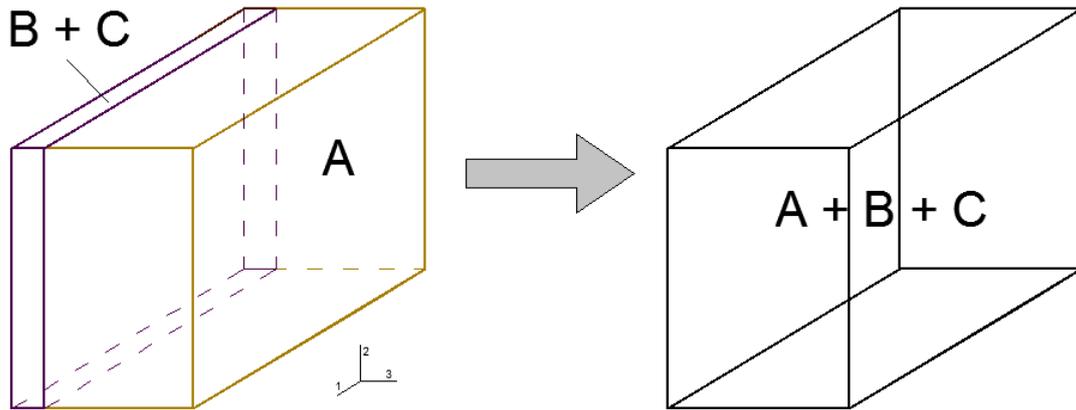- Step 4: A + B + C: the resultant parts (A and B + C) are joined,

22

Figure 18: step 4

### 3.1.1. First method: calculation of global stiffness matrix

In this procedure, for every step, the combined stiffness matrix was obtained using the rule of mixtures, component by component. In other words, the element (i,j) of the new stiffness matrix is the result of applying the rule of mixtures (choosing conveniently the formula for parallel or in series springs) to elements (i,j) of all the stiffness matrixes of the parts that are being homogenized.

Once all the steps are completed, it is possible to extract the desired parameters (E, G, and v along main directions 1, 2, and 3) from the compliance matrix, which is the inverse of the stiffness matrix. Thus, by inverting the matrix obtained after all homogenization steps, those parameters can be extracted from its elements, according to the formulation of the compliance matrix, D (figure 22).

With the values extracted from [1], the stiffness matrix for orthotropic materials (CO, figure 20) for the wood is obtained. The same procedure was applied for the bolt, but as it is made of an isotropic material, stiffness matrix in figure 21 (CI) was used. The formulation of the coefficients that form the matrices are shown below too.

$$CO = \begin{bmatrix} C_{11} & C_{12} & C_{13} & 0 & 0 & 0 \\ C_{12} & C_{22} & C_{23} & 0 & 0 & 0 \\ C_{13} & C_{23} & C_{33} & 0 & 0 & 0 \\ 0 & 0 & 0 & C_{44} & 0 & 0 \\ 0 & 0 & 0 & 0 & C_{55} & 0 \\ 0 & 0 & 0 & 0 & 0 & C_{66} \end{bmatrix}$$

Figure 19: stiffness matrix for orthotropic materials

where,

$$C_{11} = \frac{E_1 \cdot (1 - v_{23} \cdot v_{32})}{\Delta} \tag{14}$$

$$C_{12} = \frac{E_1 \cdot (v_{21} + v_{23} \cdot v_{31})}{\Delta} \tag{15}$$

$$C_{13} = \frac{E_1 \cdot (v_{31} + v_{21} \cdot v_{32})}{\Delta} \tag{16}$$

$$C_{21} = \frac{E_2 \cdot (v_{12} + v_{13} \cdot v_{32})}{\Delta} \tag{17}$$

$$C_{22} = \frac{E_2 \cdot (1 - v_{13} \cdot v_{31})}{\Delta} \tag{18}$$

$$C_{23} = \frac{E_2 \cdot (v_{12} \cdot v_{31} + v_{32})}{\Delta} \tag{19}$$

$$C_{31} = \frac{E_3 \cdot (v_{13} + v_{12} \cdot v_{23})}{\Delta} \tag{20}$$

$$C_{32} = \frac{E_3 \cdot (v_{13} \cdot v_{21} + v_{23})}{\Delta} \tag{21}$$

$$C_{33} = \frac{E_3 \cdot (1 - v_{12} \cdot v_{21})}{\Delta} \tag{22}$$

$$\Delta = 1 - v_{12} \cdot v_{21} - v_{13} \cdot v_{31} - v_{12} \cdot v_{23} \cdot v_{31} - v_{13} \cdot v_{21} \cdot v_{32} - v_{23} \cdot v_{32} \tag{23}$$

and $C_{44} = G_{23}$, $C_{55} = G_{13}$, and $C_{66} = G_{12}$.

$$CI = \begin{bmatrix} C_{11} & C_{12} & C_{12} & 0 & 0 & 0 \\ C_{12} & C_{11} & C_{12} & 0 & 0 & 0 \\ C_{12} & C_{12} & C_{11} & 0 & 0 & 0 \\ 0 & 0 & 0 & \frac{(C_{11} - C_{12})}{2} & 0 & 0 \\ 0 & 0 & 0 & 0 & \frac{(C_{11} - C_{12})}{2} & 0 \\ 0 & 0 & 0 & 0 & 0 & \frac{(C_{11} - C_{12})}{2} \end{bmatrix}$$

Figure 20: stiffness matrix for isotropic materials

where,

$$C_{11} = \frac{(1 - v) \cdot E}{(1 + v) \cdot (1 - 2v)} \tag{24}$$

$$C_{12} = \frac{v \cdot E}{(1 + v) \cdot (1 - 2v)} \tag{25}$$

Now it is necessary to generate the right stiffness matrices for each component, this is, switch the coordinate system from global coordinates to the local coordinates of each component of the composite. In figure 6 the local references are shown. In the matrix for the wooden parts,

25

the correspondence of the axis and the fibre directions are: L − 1, T − 2, R − 3. Therefore, to get the coordinate system change matrices, it is necessary to permute files according to the local references. The matrices are, for the planking and ceiling (LP), and for the frame (LP):

$$
LP = \begin{matrix}
0 & 1 & 0 & 0 & 0 & 0 \\
0 & 0 & 1 & 0 & 0 & 0 \\
1 & 0 & 0 & 0 & 0 & 0 \\
0 & 0 & 0 & 0 & 1 & 0 \\
0 & 0 & 0 & 0 & 0 & 1 \\
0 & 0 & 0 & 1 & 0 & 0
\end{matrix}
\qquad
LF = \begin{matrix}
0 & 1 & 0 & 0 & 0 & 0 \\
1 & 0 & 0 & 0 & 0 & 0 \\
0 & 0 & 1 & 0 & 0 & 0 \\
0 & 0 & 0 & 0 & 1 & 0 \\
0 & 0 & 0 & 1 & 0 & 0 \\
0 & 0 & 0 & 0 & 0 & 1
\end{matrix}
$$

Figure 21: coordinate system change matrices

Hence, the matrices CP (for the planking and ceiling) and CF (for the frame) are obtained as follows:

$$CP = LP * CW \tag{26}$$

$$CF = LF * CW \tag{27}$$

As the matrices for every component in global coordinates are calculated, it is possible to start with the homogenization. Schemes of the composite decomposition were shown in figures 15 to 19. The asterisk means that those parts are composed by smaller parts of material with different properties.

In the end, the homogenized element was obtained. From its final stiffness matrix, it can be obtained the compliance matrix (figure 23), which is the inverse of the first one.

$$D = \begin{bmatrix} \dfrac{1}{E_1} & -\dfrac{v_{12}}{E_2} & -\dfrac{v_{13}}{E_3} & 0 & 0 & 0 \\[2ex] -\dfrac{v_{21}}{E_1} & \dfrac{1}{E_2} & -\dfrac{v_{23}}{E_3} & 0 & 0 & 0 \\[2ex] -\dfrac{v_{31}}{E_1} & -\dfrac{v_{32}}{E_2} & \dfrac{1}{E_3} & 0 & 0 & 0 \\[2ex] 0 & 0 & 0 & \dfrac{1}{G_{23}} & 0 & 0 \\[2ex] 0 & 0 & 0 & 0 & \dfrac{1}{G_{31}} & 0 \\[2ex] 0 & 0 & 0 & 0 & 0 & \dfrac{1}{G_{12}} \end{bmatrix}$$

Figure 22: compliance matrix

Therefore, the parameters for the Multi – Layered Solid Wood Structure (from now, MLSWS) performing as an entity, are:

$$E_1 = \frac{1}{D\,(1,1)} \tag{28}$$

$$E_2 = \frac{1}{D\,(2,2)} \tag{29}$$

$$E_3 = \frac{1}{D\,(3,3)} \tag{30}$$

$$G_{23} = \frac{1}{D\,(4,4)} \tag{31}$$

$$G_{31} = \frac{1}{D\,(5,5)} \tag{32}$$

$$G_{12} = \frac{1}{D\,(6,6)} \tag{33}$$

$$v_{12} = -E_2 \cdot D(1,2) \tag{34}$$

$$v_{13} = -E_3 \cdot D(1,3) \tag{35}$$

$$v_{21} = -E_1 \cdot D(2,1) \tag{36}$$

$$v_{23} = -E_3 \cdot D(2,3) \tag{37}$$

$$v_{31} = -E_1 \cdot D(3,1) \tag{38}$$

$$v_{32} = -E_2 \cdot D(3,2) \tag{39}$$

### 3.1.2. Second method: calculation of global E moduli

The procedure and the steps are exactly the same they were for the previous case. The only difference is that now, the rule of mixtures is directly applied to E moduli for every component (a vector that contains $E_1$, $E_2$ and $E_3$), so the output of every step is directly the new E values, while before it was necessary extracting them from the stiffness matrix, which was the parameter that was calculated with the rule of mixtures.

Although G moduli and Poisson ratios cannot be obtained using this method, it may be still interesting to compare the values obtained for E using both ways.

## 3.2. Finite Element (FE) model

In a FE simulation, the element to analyse (in this instance, the MLSWS) is discretized, in order to let the software apply the equations at the nodes that will lead to a solution.

For this study, FE simulations were performed with the commercial software ANSYS [11] (version 16.0).

The process of building a FE model involves three phases:

- Pre-processing: all the necessary parameters (geometry, material properties, boundary conditions, etc.), are defined. In this step, the mesh can be checked to avoid convergence problems.

- Solution: after defining the load steps (the different equilibrium states of the system), the simulation runs.
- Post-processing: once the solution is done, different variables (for example, in this case, the reactions solution is wanted) can be extracted, as well as graphic representations of them.

Now, every sub – step is detailed for this case*.*

### Geometry

As the way to proceed in this text is to contrast a theoretical mechanical model with FE simulations, the geometry of the element is exactly the same for both cases. The dimensions of the element were exposed in figures 11 and 12.

### Element type

When modelling a structure with Finite Element Method, it is needed to define the kind of element to use. It is a crucial decision, as the model will be built by reproducing it and joining each other through its nodes.

The elements can differ in shape (triangular, rectangular, …), number of nodes, distribution of nodes (lagrangian, serendipity, …), mechanical formulation… In this case, the chosen element from ANSYS library was SOLID186 (see annex 1).

### Material models

The values for the wood and steel properties are the same used in chapter 1 for the mechanical model.

The wood properties were input in ANSYS choosing a linear elastic orthotropic model. Analogously, a linear elastic isotropic model was used to represent the properties of the steel of the bolt.

As stated before, and displayed in figure 6, the fibres in the planking and ceiling are orthogonally oriented with respect to the frame. The material properties showed in table 1 (recent oak) are

introduced in global ANSYS coordinates, and then local coordinate systems are created and properly assigned to each wooden part, so that the model matches the actual fibre orientation.

**Meshing**

As the dimensions of the bolt are considerably small with respect to the full MLSWS, it requires a finer mesh. However, using the same mesh size in the wooden parts, which are larger (thus, a coarser mesh is accurate enough), would lead to unnecessarily increase the number of equations and, in consequence, the calculation time. However, if the mesh size variation is too high, shape limits could be violated on the boundary of regions with different meshing.

To ensure the variation of mesh size from the bolt to the outer parts is smooth , the mesh of the wooden blocks has been divided in two, creating a finer mesh on the areas around the bolt (see figure 24). That makes the variation of the element edge length be progressive. In any case, ANSYS allows the user to check if the mesh is appropriate before solving. The mesh size was set to 12, 8 and 4 mm for the outer and inner wooden parts, and the bolt, respectively.
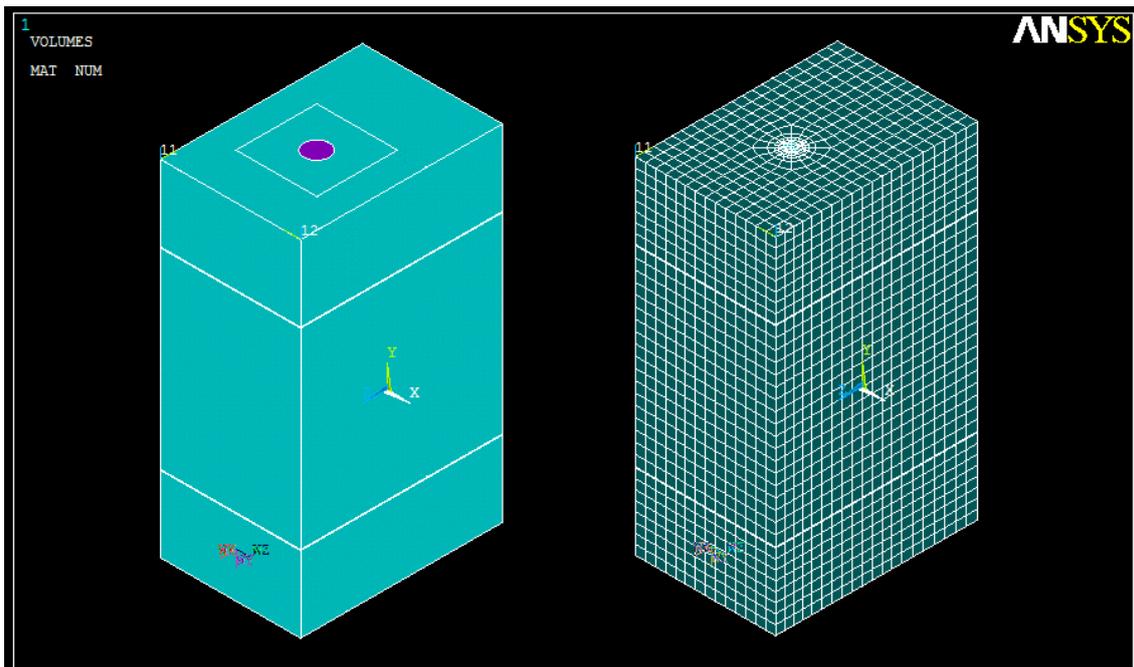


Figure 23: meshing

**Contact pairs**

The behaviour of the contact between the surfaces of the different parts of the MLSWS must be defined. The main parameters to be analysed are the friction coefficient and the contact offset.

In this case, two different types of contact are present: the contact between the different wooden components (planking – frame, and frame – ceiling) and the contact bolt – wood.

To create the contact pairs, the necessary elements to input are:

- Target and contact surfaces: normally, the biggest of both surfaces is chosen as the target surface, although it should not affect the result [12]. It must be carefully revised that all surfaces which are or will enter in contact are selected.
- Friction coefficient: it is a dimensionless scalar value which represents the ratio of the frictional force amongst two surfaces and the force they are subjected to. For the contact bolt (steel) – wood, it is recommended a value between 0.2 and 0.6, and between 0.25 and 0.6 for wood on wood [9]. For both cases, value of 0.3 was chosen, in order to be within the interval, but ensure that friction force is not overestimated. Also some references like [13] and [14] concluded that it is an acceptable value for both types of contact.
- Offset ($\delta$): also known as diametrical interference, it measures how much the contact surface penetrates in the target surface (or vice versa, if the value is negative). The value of the offset is typically about $\delta/d$ = (0.001, 0.01). Therefore, having a diameter of 28 mm in this case, and, the diametrical interference was set to 0.01 mm, which is a value within the interval, and an appropriate value suggested by [15].

**Boundary conditions and load steps**

Likewise the actual performance of the hull, where first the planks and the bolt were assembled, and afterwards different loads started acting, the finite element simulation is carried out in two stages or load steps, with the purpose of having equilibrium throughout all the calculation process. These are:

- Load step 1: the bolt is allowed to interact with the wooden parts, inducing a certain contact pressure on the surrounding surface. The boundary conditions exposed in figure 24. In the postprocessing, the stress vector $\{\sigma_0\}$ is extracted.
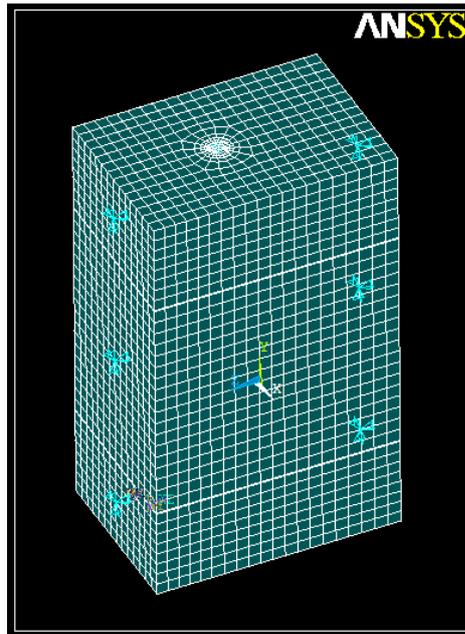
Figure 24: boundary conditions for load step 1

- Load step 2: the way to extract the desired mechanical parameters is similar to the stiffness matrix (C) method used in chapter 1. But now, each value of the matrix is extracted by applying appropriate external boundary conditions. Every column of the C matrix is calculated by setting a certain strain to $\delta/L$, being L the length of the MLSWS along the displacement direction, and making the rest of strains (and in consequence, the displacements) be zero.

These boundary conditions make possible to know the complete strain vector (see figure 26), $\{\varepsilon\}$, for every case. Like in the previous load step, when solution is done, it is possible to extract from ANSYS the components of the stress vector for this load step, $\{\sigma_1\}$.

Thereby, the stress vector, $\{\sigma\}$, due to the applied $\delta$, which from the correspondent column of C can be obtained is $\{\sigma_1\}$ - $\{\sigma_0\}$. Looking at the definition of C matrix, having the stress vector, each column can be obtained.

$$\{\sigma\} = \{C\} \cdot \{\varepsilon\}$$

$$\{\sigma\} = \begin{Bmatrix} \sigma_{11} \\ \sigma_{22} \\ \sigma_{33} \\ \sigma_{12} \\ \sigma_{13} \\ \sigma_{23} \end{Bmatrix} \qquad \{\varepsilon\} = \begin{Bmatrix} \varepsilon_{11} \\ \varepsilon_{22} \\ \varepsilon_{33} \\ 2 \cdot \varepsilon_{12} \\ 2 \cdot \varepsilon_{13} \\ 2 \cdot \varepsilon_{23} \end{Bmatrix}$$

Figure 25: strain and stress vectors

For example, being $\varepsilon_{11}$ the only not null strain, the first column of the matrix is extracted as follows:

$$\begin{bmatrix} \sigma_{11} \\ \sigma_{22} \\ \sigma_{33} \\ \sigma_{12} \\ \sigma_{13} \\ \sigma_{23} \end{bmatrix} = \begin{bmatrix} C_{11} & C_{12} & C_{13} & C_{14} & C_{15} & C_{16} \\ C_{21} & C_{22} & C_{23} & C_{24} & C_{25} & C_{26} \\ C_{31} & C_{32} & C_{33} & C_{34} & C_{35} & C_{36} \\ C_{41} & C_{42} & C_{43} & C_{44} & C_{45} & C_{46} \\ C_{51} & C_{52} & C_{53} & C_{54} & C_{55} & C_{56} \\ C_{61} & C_{62} & C_{63} & C_{64} & C_{65} & C_{66} \end{bmatrix} \cdot \begin{bmatrix} \varepsilon_{11} = \delta/L_1 \\ 0 \\ 0 \\ 0 \\ 0 \\ 0 \end{bmatrix}$$

Figure 26: obtention of the first column of C matrix

$$\sigma_{11} = C_{11} * \varepsilon_{11} \tag{40}$$

$$\sigma_{22} = C_{12} * \varepsilon_{11} \tag{41}$$

$$\sigma_{33} = C_{13} * \varepsilon_{11} \tag{42}$$

$$\sigma_{12} = C_{14} * \varepsilon_{11} \tag{43}$$

$$\sigma_{13} = C_{15} * \varepsilon_{11} \tag{44}$$

$$\sigma_{23} = C_{16} * \varepsilon_{11} \tag{45}$$

Therefore, six simulations (each for every strain vector component) are needed. However, nine were run, in order to check that $\varepsilon_{ij}$ and $\varepsilon_{ji}$ give the same result for the correspondent $G_{ij}$ and $G_{ji}$. The boundary conditions for each of them are exposed in table 4.

To calculate the three first columns, which correspond to unidirectional strain, a negative displacement (that will lead to compression, in order to ensure the members of the MLSWS keep together) of $\delta = 0.1$ mm is applied on i+ surface (this is, the surface where the value of the coordinate is higher) of the MLSWS. The normal displacement is constrained on all other surfaces.

The value of $\delta$ is reasonable as the gap between the planking and frame, and frame and ceiling is 0.001 mm in the FE model, plus the length of the composite along its shorter side is 156 mm, so the displacement is not high compared to the MLSWS dimensions, and big enough to close the gaps.

For the other three columns, that correspond to transverse stain, a positive displacement along direction j of $\delta = 0.1$ mm is set on the surface i+, letting j surfaces displace freely, and impeding normal displacements on the rest of them.

| | $\varepsilon_{11}$ | $\varepsilon_{22}$ | $\varepsilon_{33}$ | $\varepsilon_{12}$ | $\varepsilon_{13}$ | $\varepsilon_{23}$ | $\varepsilon_{21}$ | $\varepsilon_{31}$ | $\varepsilon_{32}$ |
|---|---|---|---|---|---|---|---|---|---|
| $1^+$ | $u_1 = \delta$ | $u_1 = 0$ | $u_1 = 0$ | $u_2 = \delta; u_1 = 0$ | $u_3 = \delta; u_1 = 0$ | $u_1 = 0$ | - | - | $u_1 = 0$ |
| $1^-$ | $u_1 = 0$ | $u_1 = 0$ | $u_1 = 0$ | $u_2 = 0; u_1 = 0$ | $u_3 = 0; u_1 = 0$ | $u_1 = 0$ | - | - | $u_1 = 0$ |
| $2^+$ | $u_2 = 0$ | $u_2 = \delta$ | $u_2 = 0$ | - | $u_2 = 0$ | $u_3 = \delta; u_2 = 0$ | $u_1 = \delta; u_2 = 0$ | $u_2 = 0$ | - |
| $2^-$ | $u_2 = 0$ | $u_2 = 0$ | $u_2 = 0$ | - | $u_2 = 0$ | $u_3 = 0; u_2 = 0$ | $u_1 = 0; u_2 = 0$ | $u_2 = 0$ | - |
| $3^+$ | $u_3 = 0$ | $u_3 = 0$ | $u_3 = \delta$ | $u_3 = 0$ | - | - | $u_3 = 0$ | $u_1 = \delta; u_3 = 0$ | $u_2 = \delta; u_3 = 0$ |
| $3^-$ | $u_3 = 0$ | $u_3 = 0$ | $u_3 = 0$ | $u_3 = 0$ | - | - | $u_3 = 0$ | $u_1 = 0; u_3 = 0$ | $u_2 = 0; u_3 = 0$ |

Table 2: boundary conditions

# 4. Results and discussion

## 4.1. Theoretical model

### 4.1.1. First method: calculation of global stiffness matrix

The estimation of the global parameters, according to the directions shown in figure 6 of the MLSWS (in GPa for $E_i$ and $G_{ij}$, dimensionless for $v_{ij}$) are:

| $E_1$ | | $E_2$ | | $E_3$ | |
|---|---|---|---|---|---|
| 2,44 | | 7,19 | | 5,92 | |
| $G_{12}$ | | $G_{23}$ | | $G_{13}$ | |
| 0,27 | | 0,33 | | 0,41 | |
| $v_{12}$ | $v_{21}$ | $v_{23}$ | $v_{32}$ | $v_{13}$ | $v_{31}$ |
| 0,11 | 0,32 | 0,07 | 0,06 | 0,13 | 0,32 |

Table 3: estimated mechanical properties obtained with the first method

### 4.1.2. Second method: calculation of global E moduli

After all the steps mentioned in section 3.1.2., the values, in GPa of E along the directions 1, 2 and 3 are:

| | |
|---|---|
| $E_1$ | 2,73 |
| $E_2$ | 7,15 |
| $E_3$ | 6,09 |

Table 4: estimated mechanical properties obtained with the second method

It can be seen that the Young's moduli values for both methods are pretty close, which gives more reliability to the theoretical model.

## 4.2. Finite Element (FE) model

Once the C matrix is built, Young's and Shear moduli and Poisson's ratios are calculated with the formulas exposed in x in chapter x.

The results (in GPa for $E_i$ and $G_{ij}$, dimensionless for $v_{ij}$) for the three directions displayed in figure 6 are shown in table 5.

| $E_1$ | | $E_2$ | | $E_3$ | |
|---|---|---|---|---|---|
| 4,17 | | 7,65 | | 6,15 | |
| $G_{12}$ | | $G_{23}$ | | $G_{13}$ | |
| 0,15 | | 0,47 | | 0,24 | |
| $v_{12}$ | $v_{21}$ | $v_{23}$ | $v_{32}$ | $v_{13}$ | $v_{31}$ |
| 0,14 | 0,26 | 0,07 | 0,06 | 0,18 | 0,27 |

Table 5: estimated global parameters extracted from the FE model

Note that it is was assumed that real values can differ quite much to this estimation, due to the unpredictable behaviour of the hull composite, caused by the sensitivity of timber to environmental changes (such as moisture, temperature,…), bolt-timber contact, layers interaction,…

It can be seen that Young's modulus along the direction of the bolt ($E_1$) is considerably higher than the value obtained for the theoretical model. This is due to the friction between the bolt and the wooden planks, fact that has only been introduced in the FE model.

In addition, $E_2$ and $E_3$ values obtained in the FE simulations are a bit higher. The reason is the press fit created by the insertion of the bolt in a slightly smaller hole, generating stress in the plane that is perpendicular to the bolt (see annex 2).

For the same reason, the shear modulus when transverse deformation appears on that plane is much higher in the FE analysis. However, the other two shear moduli are lower compared to the

theoretical model; this can be explained taking into account the different components of the MLSWS are not fixed to each other.

# 5. Conclusions

From the work achieved during this dissertation work it is possible to conclude that the main objectives have been satisfied. The difference between the results obtained by both methods can be considered acceptable regarding the assumptions and limitations of each of them.

This study let me understand the crucial parameters that can affect the results of a Finite Element analysis. Furthermore, building a theoretical estimation with Matlab helped me to understand the basics of mechanics, as I could see the evolution of the parameters step by step.

In addition, being the work framed in a bigger project, gave me the opportunity to learn and have very interesting feedback from experienced people, that would had never acquired by doing an independent work.

# 6. Future work

The outcome of this text can be contrasted with the upcoming results of laboratory tests of the manufactured samples created for the Vasa research team's study and Claudia Vara's dissertation.

In addition, this work is intended to help to the understanding of the mechanical behaviour of Vasa vessel, which is the goal of the Vasa research team at Uppsala University, in order to facilitate the design of a new support structure for the ship. The Vasa project deadline is December 2016.

Starting from the *super-element* that has been proposed, another interesting study would be how the dowel and bolt density can affect the mechanical response of the whole ship structure.

# 7. Acknowledgements

# References

[1] Muñoz García M., Hurtado Sierra J.C., *Structural analysis of the 17th century warship Vasa*, University of Skövde, Master Thesis, 2014.

[2] http://www.vasamuseet.se/en/The-Ship/The-sinking/

[3] Dabbagh A., Garza C., *Finite element analysis of the Vasa's bottom structure*, Master Thesis, University of Skövde, 2011.

[4] Bommier F., *Towards a detailed computational model of the Vasa ship – Analysis of its mechanical connections*, Uppsala Universitet, Master Thesis, 2014.

[5] Sandvik, *Möt Sandvik Juni 2011*, Spoon Publishing, 2011.

[6] Gürdal Z., Haftka R. T., Hajela P., *Design and Optimization of Laminated Composite Materials*, FP Innovations, 1999.

[7] Whitcomb J., Noh J., *concise derivation of formulas for 3D sublaminate homogenization*, J Compos Mater, 2000.

[8] Sandvik, *Sandvik SAF 2707 HD*, 2011.

[9] Pero-Sanz Elorza, J.A., *Ciencia e ingeniería de los materiales*, CIE Dossat, 2006.

[10] Matlab, *Matlab Primer*, 2013.

[11] ANSYS Inc., *ANSYS Mechanical User's Guide*, ANSYS Inc., 2013.

[12] Oñate, E., *Cálculo de estructuras por el Método de Elementos Finitos*, CIMNE, 1993.

[13] Koubek R., Dedicova K., *Friction of wood on steel*, Linnaeus University, Master Thesis, 2014.

[14] Aira J.R., Arriaga F., Íñiguez – González G., Crespo J., *Static and kinetic friction coefficients of Scots pine (Pinus sylvestris L.), parallel and perpendicular to grain direction*, 2013.

[15] van Beek, A., *Advanced Engineering Design*, Delft University of Technology, 2015.

# Annex 1: Type of finite element selected

The chosen ANSYS library element for modelling both the bolt and the wooden layers is SOLID186. It is a three-dimensional element, with 20 nodes and quadratic shape functions. It has three degrees of freedom at each node: x,y, and z nodal displacements. Mechanically, it supports hyperelasticity, plasticity, and creep, amongst other features, so that is enough to model properly the case of study in this work. A scheme of SOLID186 element can be seen in figure 30.
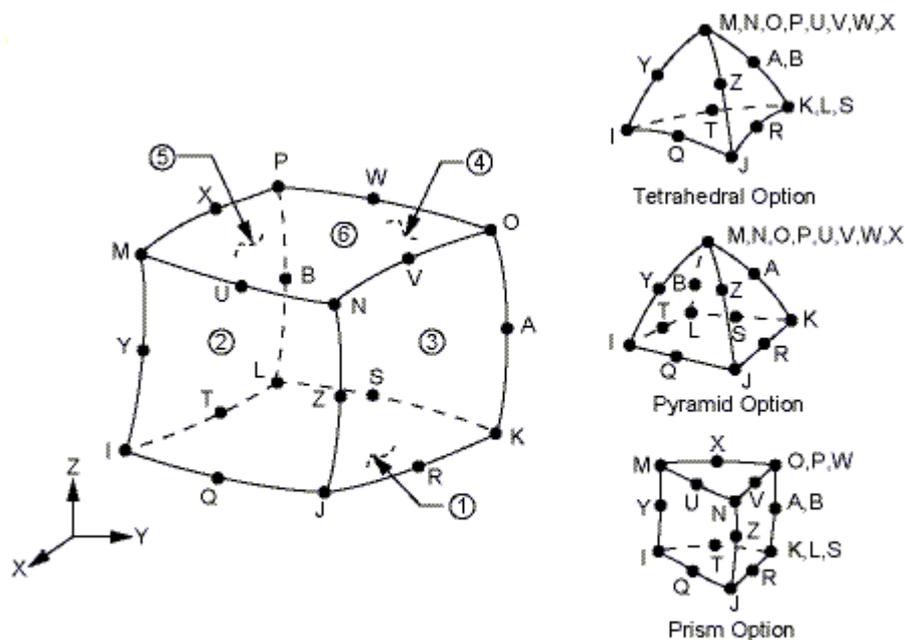


Figure 27. Credits: ANSYS

SOLID186 can be obtained in two forms: homogeneous structural solid, and layered structural solid. Although this case is a composite with different layers, the first option was chosen, as there are initial gaps between the different layers, so if they are considered, it is required to have independent bodies for each plank.

# Annex 2: study of the influence of the bolt press fit

The diametrical interference between the bolt and the wood that surrounds it adds extra stiffness to the element. This fact was not considered in the theoretical model built in chapter 1, therefore different simulations, for diverse offset values, were performed, in order to analyse the relationship amongst stiffness and different offset configurations.

The geometry is the same used in the previous FE calculations, and the material model, for the MLSWS, is isotropic, with a stiffness of 5000 MPa and a Poisson's ratio of 0.4 (values that are within the range of oak, the main material in this case).

The reason of choosing this simple material model is to avoid facts that could provoke any other variations in the results other than the induced by the contact pressure the insertion of the bolt creates, thereby it is possible to analyse the influence this fact has in the stiffness of the MLSWS. Thus, in the graphics below, the vertical axis represents the percentage of variation of the Young's modulus with respect to a similar model without press fit.

For all directions, the stiffness increases when a higher value for the diametrical interference is set. For 1-axis (parallel to the bolt, as was displayed in figure 6), notice that, despite it raises, as shown in figure 27 the stiffness is always lower than 5000 MPa (the expected value if the sample was homogeneous).
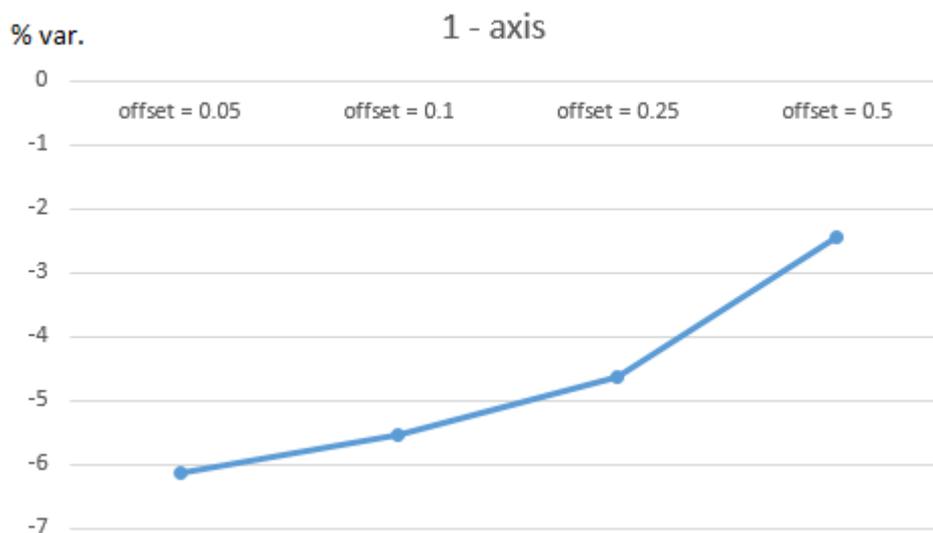


Figure 28: influence of different offsets for axis 1

The main reason for this is the discontinuity the bolt creates, and the contact pressure only appears in planes which are normal to the cylinder axis. Hence, for 2 and 3-axis, the stiffness is always higher than the introduced value for the material. In addition, the growth is much higher and, as might be expected based on the geometry, very similar for these axes (see figures 28 and 29).
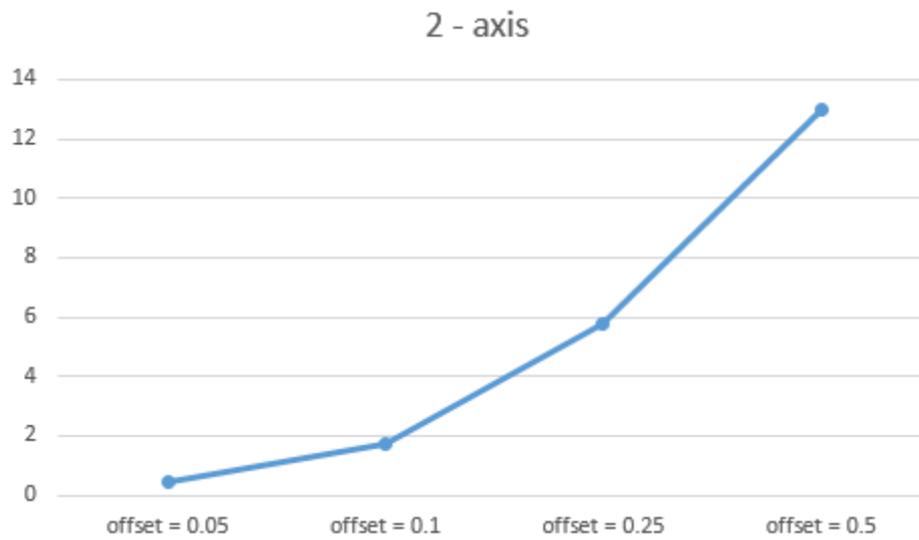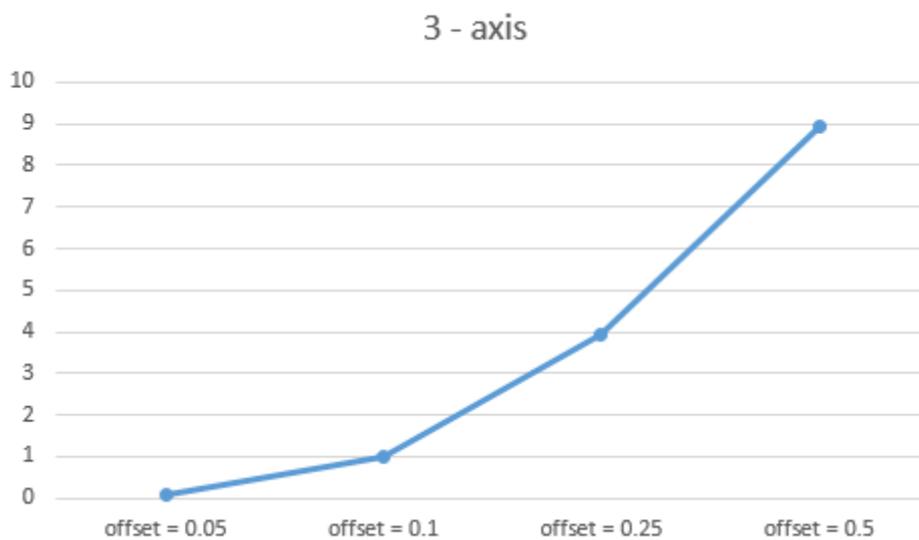


*Figure 29 influence of different offsets for axis 2*



Figure 30 influence of different offsets for axis 3